Available online at www.sciencedirect.com
SCIENCE DIRECT®
ELSEVIER
International Journal of Mechanical Sciences 46 (2004) 1213–1231
International Journal of MECHANICAL SCIENCES
www.elsevier.com/locate/ijmecsci

Eigenanalysis and continuum modelling of an asymmetric beam-like repetitive structure

N.G. Stephen*, Y. Zhang

School of Engineering Sciences, Mechanical Engineering, University of Southampton, Highfield, Southampton SO17 1BJ, UK

Received 20 October 2003; received in revised form 16 June 2004; accepted 18 July 2004

Abstract

An asymmetric repetitive pin-jointed structure, based upon a 3-D *NASA* framework, is analysed using a state variable transfer matrix technique. A conventional transfer matrix cannot be constructed due to the singularity of one partition of the stiffness matrix; instead, a cell (rather than cross-sectional) state vector consisting of displacements only is employed, leading to a generalised eigenvalue problem. The asymmetry of the structure leads to tension–torsion and bending–shear couplings, which may be explained in terms of the tension–shear coupling of a single face of the structure. Equivalent continuum beam properties and coupling coefficients are determined, and the effect of (a)symmetry discussed as a trade between, for example, tension-Poisson's ratio contraction for a symmetric structure, against tension–torsion coupling for the asymmetric.

Keywords: Repetitive; Asymmetric; Pin-jointed structure; Transfer matrix; Eigenanalysis; Equivalent continuum properties; Tension–torsion coupling

1. Introduction

In this paper, a repetitive asymmetric pin-jointed structure modelled on a *NASA* deployable satellite boom [1] is treated by eigenanalysis. Such structures have previously been analysed [2] as

*Corresponding author. Tel.: +44-23-8059-2359; fax: +44-23-8059-3230.
E-mail address: ngs@soton.ac.uk (N.G. Stephen).

0020-7403/$ - see front matter
doi:10.1016/j.ijmecsci.2004.07.012

Nomenclature

A	cross-sectional area
A, **B**	matrices of the generalised eigenvalue problem
d	member diameter
d	nodal displacement vector
E	Young's modulus
F	force vector
G	shear modulus
G	transfer matrix
H	height of *cell* cross-section ($H = \sqrt{3}L/2$)
I	second moment of area
I	identity matrix
J	torsion constant
J	Jordan block matrix, canonical form
K	coupling coefficient
K	stiffness matrix
L	length of longitudinal members
M	moment
n	index of cell or section, element of **N**
N	compliance matrix
Q	shearing force
R	radius of bending curvature ($1/R = \partial\psi/\partial x$)
s	state vector
t	column vector of **T**
T	tensile force
T	*transmission* matrix
u, v, w	displacements in the x-, y- and z-directions, respectively
v	eigenvector
V	transformation matrix of eigen- and principal vectors
w	principal vector
x, y, z	cartesian coordinate system

Greek letters

γ	shear angle
ε	direct strain
θ	rotation (twist) about the x-axis
κ	shear coefficient
λ	eigenvalue
ν	Poisson's ratio
ψ	cross-sectional rotation

an eigenproblem of a state vector transfer matrix: the stiffness matrix **K** for a typical repeating cell is constructed first, and relates nodal force and displacement components as

$$\begin{bmatrix} \mathbf{F}_L \\ \mathbf{F}_R \end{bmatrix} = \begin{bmatrix} \mathbf{K}_{LL} & \mathbf{K}_{LR} \\ \mathbf{K}_{RL} & \mathbf{K}_{RR} \end{bmatrix} \begin{bmatrix} \mathbf{d}_L \\ \mathbf{d}_R \end{bmatrix}. \tag{1}$$

The transfer matrix **G** is then

$$\begin{bmatrix} \mathbf{d}_R \\ \mathbf{F}_R \end{bmatrix} = \begin{bmatrix} -\mathbf{K}_{LR}^{-1}\mathbf{K}_{LL} & -\mathbf{K}_{LR}^{-1} \\ \mathbf{K}_{RL} - \mathbf{K}_{RR}\mathbf{K}_{LR}^{-1}\mathbf{K}_{LL} & -\mathbf{K}_{RR}\mathbf{K}_{LR}^{-1} \end{bmatrix} \begin{bmatrix} \mathbf{d}_L \\ -\mathbf{F}_L \end{bmatrix}, \tag{2}$$

or, more compactly, $\mathbf{s}_R = \mathbf{G}\mathbf{s}_L$, where the state vectors consist of the nodal displacement and force components on the left- and right-hand sides (subscripts L and R) of the single cell. An eigenvector describes a fixed pattern of displacement and force components which is unique to within a scalar multiplier; translational symmetry demands that this pattern is preserved as one moves from cell to cell, allowing one to write $\mathbf{s}_R = \lambda\mathbf{s}_L$, which leads to the standard eigenvalue problem $\mathbf{G}\mathbf{s}_L = \lambda\mathbf{s}_L$, or $(\mathbf{G} - \lambda\mathbf{I})\mathbf{s}_L = \mathbf{0}$. Non-unity eigenvalues of **G** occur as reciprocals, and are the Saint-Venant decay rates pertaining to self-equilibrated end loading. Multiple unity eigenvalues pertain to the transmission modes of tension, torsion, bending moment and shear, together with the rigid body displacements and rotations. From a knowledge of the eigen- and principal vectors associated with the unity eigenvalues, equivalent continuum beam properties of cross-sectional area, Poisson's ratio, second moment of area, torsion constant and shear coefficient may be calculated. The example chosen in [2] was pin-jointed, as the finite element analysis (FEA) of such structures involves only exact elements, so predictions from the eigenanalysis may be verified by comparison with what may be regarded as exact FEA results.

For the pin-jointed idealisation of the example structure [1], matrix $\mathbf{K}_{LR}$ is singular, so the transfer matrix as defined above cannot be constructed; instead the approach is redefined as a generalised eigenvalue problem, with vectors consisting of the displacement components on both sides of the cell, rather than displacement and force on one side. Beside the 12 unity eigenvalues for the transmission modes, eigenanalysis of the structure shows three eigenvalues equal to zero, and three equal to infinity since they must occur as reciprocals. This implies that any self-equilibrated load is confined to the cross-section on which it is applied, and does not penetrate into the structure; indeed, this is precisely why the matrix partition is singular—nodal displacement components on the right-hand side of the cell are quite unaffected by some force components applied at nodes on the left-hand side of the cell, resulting in a complete row and column of zeros within the matrix partition.

Since the eigen- and principal vectors of the generalised problem contain only displacement components, a *transmission* matrix **T** is defined, consisting of transmission vectors of both displacement and force components. Physical interpretation of the vectors in **T** shows coupling between various modes of displacement; tension is coupled with torsion, which is reminiscent of the established behaviour of pre-twisted beams, while pure bending is coupled to a shear deflection perpendicular to the plane of curvature, with a reciprocal coupling for a shearing force (Fig. 1).

Finally, we note that Noor [3] has provided a review and classification of the approaches to the analysis of repetitive structures, and the present work represents a combination of his *periodic*

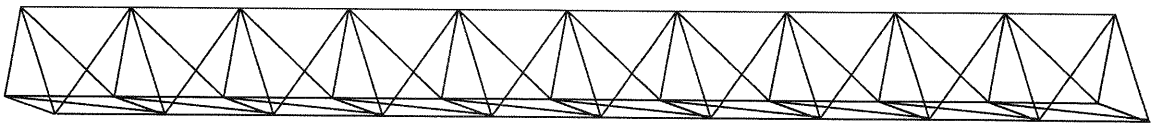

Fig. 1. A ten-cell asymmetric 3-D pin-jointed framework having equilateral triangular cross-section.

structure method in order to determine the relevant properties for his *substitute continuum method.* Earlier, Sun and Kim [4] simulated static loading, numerically, in order to effectively measure the equivalent properties of a typical cell of the lattice; however that approach required a prior knowledge of the magnitude and distribution of the nodal forces, and also boundary constraints must be carefully specified to allow, for example, Poisson's ratio effects in a simulation of tension. More recently, Lee [5] has employed equality of kinetic and strain energies of a typical cell, to that of a finite element model of an equivalent continuum, and noted that natural frequency predictions were an overestimate compared to conventional FEA; one would expect as much, since the fewer continuum degrees of freedom implies additional constraints and hence increased frequency according to Rayleigh's principle.

2. Generalised eigenvalue problem

Consider two consecutive cells of the 3-D framework shown in Fig. 2; let $\mathbf{d}_{n-1}$, $\mathbf{d}_n$ and $\mathbf{d}_{n+1}$ denote the nodal displacement vectors associated with the $(n-1)$th, nth, and $(n+1)$th sections, respectively. The corresponding nodal force vectors $\mathbf{F}_{n-1}$, $\mathbf{F}_n$ and $\mathbf{F}_{n+1}$ are related to the displacements through the equations

$$\begin{bmatrix} \mathbf{F}_{n-1} \\ \mathbf{F}_n \end{bmatrix} = \mathbf{K} \begin{bmatrix} \mathbf{d}_{n-1} \\ \mathbf{d}_n \end{bmatrix} \quad \text{and} \quad \begin{bmatrix} \mathbf{F}_n \\ \mathbf{F}_{n+1} \end{bmatrix} = \mathbf{K} \begin{bmatrix} \mathbf{d}_n \\ \mathbf{d}_{n+1} \end{bmatrix}, \tag{3a,b}$$

where $\mathbf{K}$ has partitions as in Eq. (1). The force component $\mathbf{F}_n$ appears in both of the relationships for the two adjacent cells, and can be eliminated to give

$$\mathbf{K}_{RL}\mathbf{d}_{n-1} + (\mathbf{K}_{LL} + \mathbf{K}_{RR})\mathbf{d}_n + \mathbf{K}_{LR}\mathbf{d}_{n+1} = \mathbf{0}. \tag{4}$$

Define displacement state vectors for adjacent cells as $\mathbf{s}_n = [\mathbf{d}_{n-1}^{\mathrm{T}}\ \mathbf{d}_n^{\mathrm{T}}]^{\mathrm{T}}$ and $\mathbf{s}_{n+1} = [\mathbf{d}_n^{\mathrm{T}}\ \mathbf{d}_{n+1}^{\mathrm{T}}]^{\mathrm{T}}$, so (4) can be expressed as

$$\mathbf{A}\mathbf{s}_n = \mathbf{B}\mathbf{s}_{n+1}, \tag{5}$$

where

$$\mathbf{A} = \begin{bmatrix} \mathbf{0} & \mathbf{I} \\ -\mathbf{K}_{RL} & -\mathbf{K}_{RR} \end{bmatrix}, \quad \mathbf{B} = \begin{bmatrix} \mathbf{I} & \mathbf{0} \\ \mathbf{K}_{LL} & \mathbf{K}_{LR} \end{bmatrix}, \tag{6a,b}$$

and $\mathbf{I}$ is the identity matrix. Now set

$$\mathbf{s}_{n+1} = \lambda \mathbf{s}_n, \tag{7}$$

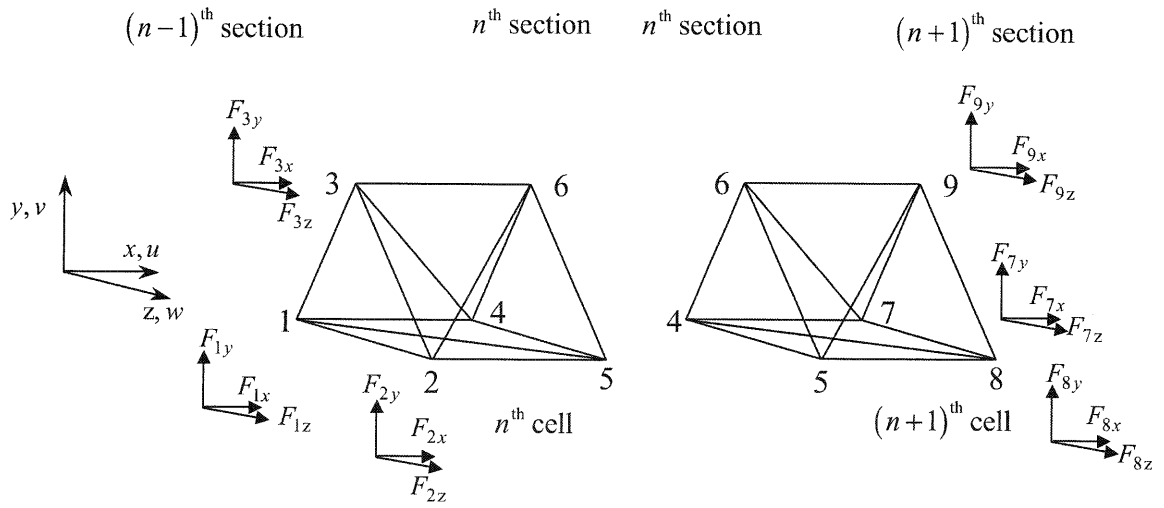

Fig. 2. Two consecutive nth and $(n+1)$th cells of the framework shown in Fig. 1.

to give the generalised eigenvalue problem

$$\mathbf{A}\mathbf{s}_n = \lambda\mathbf{B}\mathbf{s}_n, \quad \text{or} \quad (\mathbf{A} - \lambda\mathbf{B})\mathbf{s}_n = \mathbf{0}. \tag{8a,b}$$

Eigenvectors for the non-repeating eigenvalues are determined from the MATLAB *eig* command. The principal vectors are determined from the near diagonalised form

$$\mathbf{A}\mathbf{V} = \mathbf{B}\mathbf{V}\mathbf{J}, \tag{9}$$

where $\mathbf{V}$ is the similarity matrix of eigen- and principal vectors, and $\mathbf{J}$ is the Jordan canonical form (JCF). For the multiple unity eigenvalues this implies the chain of equations

$$\begin{aligned} (\mathbf{A} - \mathbf{B})\mathbf{v}_1 &= \mathbf{0} \\ (\mathbf{A} - \mathbf{B})\mathbf{w}_2 &= \mathbf{B}\mathbf{v}_1 \\ &\cdots\cdots\cdots\cdots \\ (\mathbf{A} - \mathbf{B})\mathbf{w}_k &= \mathbf{B}\mathbf{w}_{k-1} \end{aligned} \tag{10a–k}$$

for a Jordan block of size $k \times k$, and a principal vector $\mathbf{w}_{i+1}$ is found using the reduced row echelon form (*rref*) command on the augmented matrix $[\mathbf{A} - \mathbf{B}, \mathbf{B}\mathbf{w}_i]$. In fact the JCF cannot be determined numerically through a similarity transformation, since matrix $\mathbf{B}$ cannot be inverted; however, the structure of the Jordan blocks for the vectors pertaining to the unity eigenvalues are obvious through physical reasoning: thus one has a 2×2 block coupling extension and the combination of loads necessary to produce that extension, and likewise a 2×2 block coupling rotation (twist) and the loads necessary to produce that rotation. On the other hand, one has two 4×4 blocks coupling transverse displacement, rotation, bending, and shear in two planes.

Since the eigen- and principal vectors consist of displacement components only, a *transmission* matrix $\mathbf{T}$ is defined, consisting of vector pairs $\mathbf{t}_{n-1} = [\mathbf{d}_{n-1}^{\mathrm{T}} \ -\mathbf{F}_{n-1}^{\mathrm{T}}]^{\mathrm{T}}$ and $\mathbf{t}_n = [\mathbf{d}_n^{\mathrm{T}} \ \mathbf{F}_n^{\mathrm{T}}]^{\mathrm{T}}$, which are derived from two of the vectors coupled in the above chain, for example $\mathbf{w}_{k-1}$ and $\mathbf{w}_{k-2}$. The force components within the new vectors can be readily determined through Eq. (1). Column pairs of $\mathbf{T}$

describe the displacement and force components on the left- and right-hand sides of a single repeating cell for the transmission of the stress resultants of tension, torsion, bending moments and shearing forces, together with the principal vector rigid body rotations; the generating eigen- and principal vectors describing rigid body displacements and rotation reside within the second vector of the pair.

3. The asymmetric *NASA* framework

The framework has material and geometric properties as follows: Young's modulus $E = 70 \times 10^9\,\mathrm{N\,m^{-2}}$, member diameter $d = 6.35\,\mathrm{mm}$; the longitudinal bars have length $L = 342.8\,\mathrm{mm}$ and cross-sectional area $A = \pi d^2/4$. The lengths of the (equilateral triangular) cross-sectional bars are also L, but their cross-sectional areas are taken as $A/2$, since they are regarded as being shared by adjacent cells, while the diagonal bars within the faces of the cell have length $\sqrt{2}L$, together with cross-sectional area A.

3.1. Eigenvalues

The QR algorithm within the MATLAB command *eig* returns the reciprocal eigenvalue pairs $[\mathrm{inf}, 0]^{\mathrm{T}}$ having multiplicity of three, implying that any self-equilibrated load applied to the left- or right-hand end of the structure does not penetrate into the structure, together with 12 eigenvalues very close to unity; physically, the latter must be exactly equal to unity and the associated eigen- and principal vectors describe the three rigid body translations in the x-, y- and z-directions, and three rigid body rotations about these axes, and six transmitting modes of tension, torsion, and bending moments and shearing forces in both the xy- and xz-planes.

3.2. Eigenvectors associated with unity eigenvalues

For $\lambda = 1$, the set of equations

$$(\mathbf{A} - \mathbf{B})\mathbf{v}_i = \mathbf{0} \tag{11}$$

and use of the *rref* command within MATLAB, gives the four independent eigenvectors—rigid body displacements in the x-, y-, and z-directions and a rigid body rotation about the x-axis. These are

$$\mathbf{v}_{rigidx} = [1\,0\,0\,1\,0\,0\,1\,0\,0\,1\,0\,0\,1\,0\,0\,1\,0\,0]^{\mathrm{T}} \times 10^{-8},$$

$$\mathbf{v}_{rigidy} = [0\,1\,0\,0\,1\,0\,0\,1\,0\,0\,1\,0\,0\,1\,0\,0\,1\,0]^{\mathrm{T}} \times 10^{-8},$$

$$\mathbf{v}_{rigidz} = [0\,0\,1\,0\,0\,1\,0\,0\,1\,0\,0\,1\,0\,0\,1\,0\,0\,1]^{\mathrm{T}} \times 10^{-8},$$

$$\mathbf{v}_{rotx} = \left[0\ \frac{L\theta}{2}\ -\frac{H\theta}{3}\ 0\ -\frac{L\theta}{2}\ -\frac{H\theta}{3}\ 0\ 0\ \frac{2H\theta}{3}\ 0\ \frac{L\theta}{2}\ -\frac{H\theta}{3}\ 0\ -\frac{L\theta}{2}\ -\frac{H\theta}{3}\ 0\ 0\ \frac{2H\theta}{3}\right]^{\mathrm{T}}, \tag{12a, b, c, d}$$

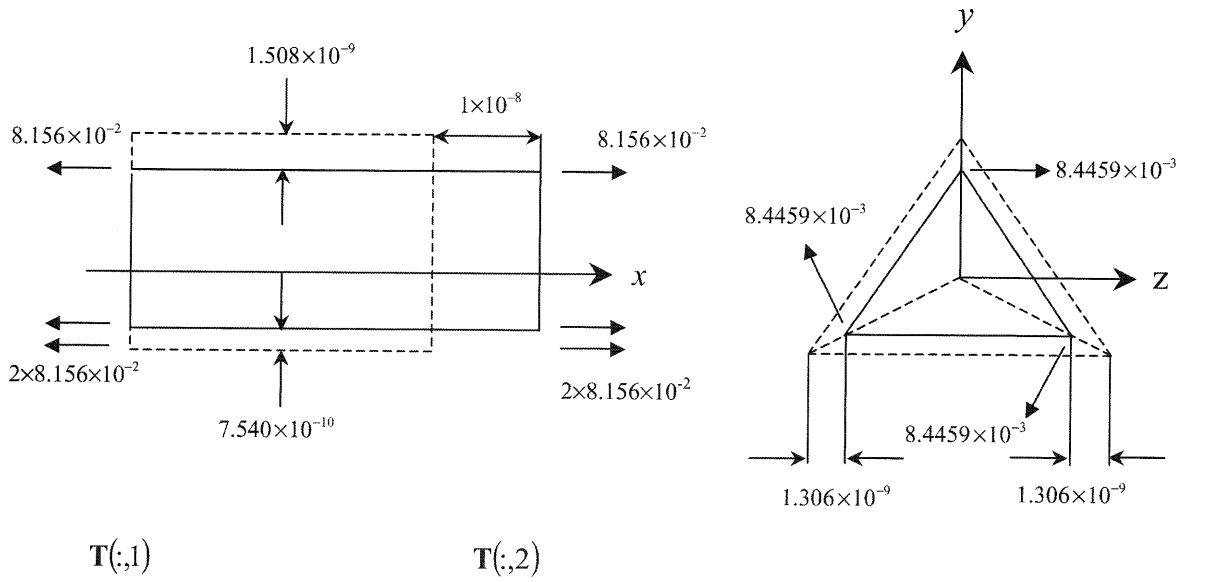

Fig. 3. Cell subject to tension and twisting moment producing pure extension, and an apparent Poisson's ratio contraction; vectors **T**(:,1) and **T**(:,2) describe the displacement and force components on the left- and right-hand side of the cell, respectively.

where L is both the length of the cell, and the length of the members which make up the cross-section, and H is the height of the cell; the small angle θ is arbitrarily chosen to be 5×10^{-8} rad.

3.3. *Transmission vectors associated with unity eigenvalues, and equivalent continuum properties*

The coupled principal vectors are determined according to the procedures described in Section 2, from which the transmission vectors are calculated, as listed in Appendix A.

3.3.1. *Extension pair*

The first two columns of the transmission matrix,[1] $\mathbf{T}(:,1)$ and $\mathbf{T}(:,2)$, are derived from the principal vector coupled to rigid body displacement in the x-direction in the principal vector chain. From Fig. 3, it is seen that a combination of tensile force $T = 2.447 \times 10^{-1}$ N and twisting moment $M_x = -5.015 \times 10^{-3}$ N m, when applied to both the left- and right-hand sides of the cell, produces an extension $u = 1 \times 10^{-8}$ m.

3.3.2. *Torsional rotation pair*

The third and fourth columns of the transmission matrix, $\mathbf{T}(:,3)$ and $\mathbf{T}(:,4)$, are derived from the principal vector coupled to rigid body rotation about the x-axis in the principal vector chain; from Fig. 4 it is seen that a combination of twisting moment $M_x = 2.481 \times 10^{-3}$ N m and

[1]Column vectors of the transmission matrix **T** are identified using the MATLAB syntax.

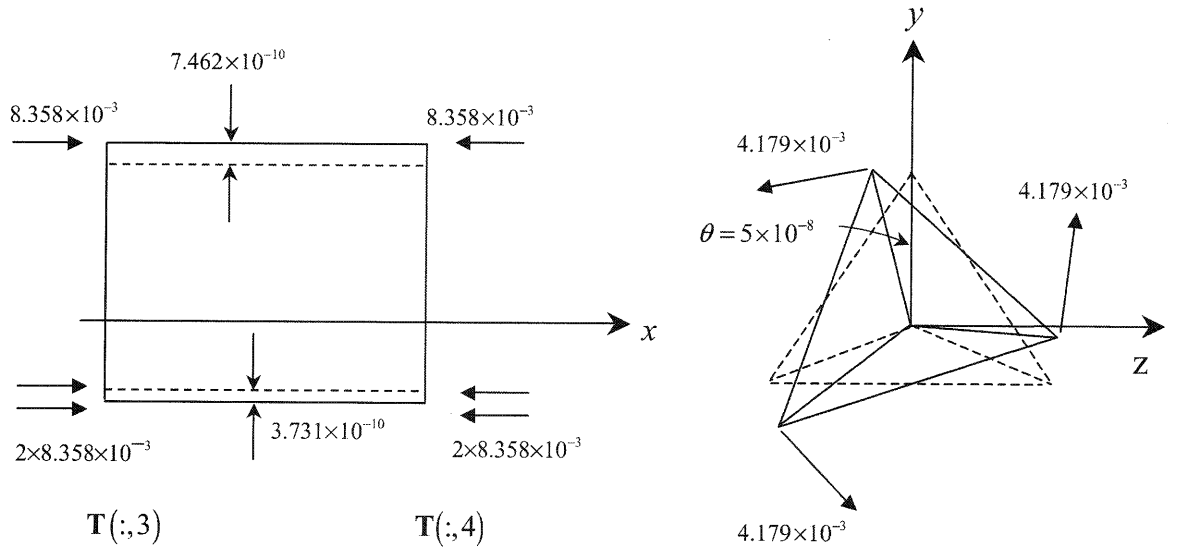

Fig. 4. Cell subjected to twisting moment and compressive force producing pure rotation about the x-axis, and an apparent Poisson's ratio expansion; vectors $\mathbf{T}(:,3)$ and $\mathbf{T}(:,4)$ describe the displacement and force components on the left- and right-hand side of the cell, respectively.

compressive force $T = -2.507 \times 10^{-2}$ N, when applied to the left- and right-hand sides of the cell, produces a pure rotation of $\theta = 5 \times 10^{-8}$.

For an equivalent continuum, the above tension–torsion coupling may be written in matrix form

$$\begin{bmatrix} T \\ M_x \end{bmatrix} = \begin{bmatrix} EA & K_{tt} \\ K_{tt} & GJ \end{bmatrix} \begin{bmatrix} \partial u/\partial x \\ \partial\theta/\partial x \end{bmatrix}, \tag{13}$$

where K_{tt} is the tension–torsion coupling coefficient. From the *extension pair*, one knows T, M_x, L and E, and $\partial u/\partial x = u/L = 2.917 \times 10^{-8}$; in particular one has $\partial\theta/\partial x = 0$, and substitution into (13) gives $T = EA(\partial u/\partial x)$, or $A = T/(E\,\partial u/\partial x) = 119.8 \times 10^{-6}\,\mathrm{m}^2$, and $M_x = K_{tt}(\partial u/\partial x)$, or $K_{tt} = M_x/(\partial u/\partial x) = -1.719 \times 10^5\,\mathrm{N\,m}$. Also in Fig. 3, one sees displacements in the y- and z-directions, suggesting an *apparent* Poisson's ratio contraction of the cross-section, calculated as follows: strain in the x-direction is $\varepsilon_x = u/L = 2.917 \times 10^{-8}$, while strain in the y-direction is $\varepsilon_y = -v/H = -(d_{1y} - d_{3y})/H = -7.620 \times 10^{-8}$ and strain in the z-direction is $\varepsilon_z = -w/L = -(d_{1z} - d_{2z})/L = -7.620 \times 10^{-8}$. Writing $\varepsilon_y = -\nu\varepsilon_x$, $\varepsilon_z = -\nu\varepsilon_x$, gives the apparent equivalent Poisson's ratio $\nu = 0.2612$. Coincidentally, if one calculates the actual cross-sectional area of the three longitudinal members in the cell as $A_{actual} = 3 \times \pi d^2/4 = 95.01 \times 10^{-6}\,\mathrm{m}^2$, one sees that the equivalent cross-sectional area as calculated above is numerically equal to $A_{actual}(1 + \nu)$. Also an equivalent shear modulus could be calculated as $G = E/[2(1 + \nu)] = 27.75 \times 10^9\,\mathrm{N\,m}^{-2}$; on the other hand, should Poisson's ratio be zero, one would have simply $G = E/2 = 35 \times 10^9$.

From the *torsional rotation pair*, vectors $\mathbf{T}(:,3)$ and $\mathbf{T}(:,4)$, one knows T, M_x, L and E, and $\partial\theta/\partial x = \theta/L = 1.459 \times 10^{-7}$; in particular one has $\partial u/\partial x = 0$, and (13) gives $M_x = GJ(\partial\theta/\partial x)$, or $J = M_x/[G(\partial\theta/\partial x)] = 4.860 \times 10^{-7}\,\mathrm{m}^4$, where $G = 35 \times 10^9$ has been employed, and $T = K_{tt}(\partial\theta/\partial x)$, or $K_{tt} = T/(\partial\theta/\partial x) = -1.719 \times 10^5\,\mathrm{N\,m}$. Note that identical coupling coefficients are obtained from the two separate vector pairs, as one would expect from the reciprocal theorem. At first sight, this pair also suggests a Poisson's ratio effect: the combination of twisting moment and compressive force necessary to produce rotation, but no extension, results in a cross-sectional expansion, Fig. 4; however since the strain in the x-direction is zero, an equivalent Poisson's ratio from this vector pair would have to be infinite.

These apparent (and inconsistent) Poisson's ratio effects arise because in each case the cell is subjected to a combined loading; however, moduluses of elasticity for a continuum, according to Love [6, article 73], should be calculated from the strains (here displacements) produced by a single stress (here single force or moment). Accordingly, combine the extension and torsional rotation vector pairs in appropriate proportion to generate *tension* and *torsion* pairs. The former describes the coupled extension and rotation produced by just a tensile force, the latter describes the coupled extension and rotation produced by just a twisting moment; these revised vectors are given in Appendix B. To determine the equivalent continuum properties from these pairs requires Eq. (13) to be expressed in its inverted form

$$\begin{bmatrix} \partial u/\partial x \\ \partial\theta/\partial x \end{bmatrix} = \begin{bmatrix} n_{11} & n_{12} \\ n_{21} & n_{22} \end{bmatrix} \begin{bmatrix} T \\ M_x \end{bmatrix} = \mathbf{N} \begin{bmatrix} T \\ M_x \end{bmatrix}, \tag{14}$$

where

$$\mathbf{N} = \begin{bmatrix} EA & K_{tt} \\ K_{tt} & GJ \end{bmatrix}^{-1} \tag{15}$$

is now a compliance matrix. Instead of one of the displacements being zero, as in the previous vector pairs, now the twisting moment and tensile force are zero in turn, from which one may easily calculate $n_{11} = 15.04 \times 10^{-8}$, $n_{12} = n_{21} = 1.519 \times 10^{-6}$ and $n_{22} = 7.414 \times 10^{-5}$; inverting the compliance matrix then gives identical equivalent properties to those calculated previously. The left-hand column of the *tension* pair shows that all nodal displacements on the left-hand side of the cell are zero, while the nodal displacements on the right-hand side consists of the extension $u = 1 \times 10^{-8}\,\mathrm{m}$, together with nodal displacements equivalent to a cross-sectional rotation of $\theta = 2\sqrt{3}/L \times 10^{-8} = 3/H \times 10^{-8}$ indicating the relationship $u = H\theta/3$; however, there are no displacements (on either side of the cell) consistent with a cross-sectional contraction, confirming that the equivalent Poisson's ratio is actually zero.

3.3.3. *Rigid rotation pairs*

The fifth and sixth columns of the *transmission matrix* $\mathbf{T}(:,5)$ and $\mathbf{T}(:,6)$ are determined from the principal vector describing rigid body rotation about the z-axis, which is coupled to rigid body displacement in the y-direction, in the principal vector chain. Similarly, the 11th and 12th columns $\mathbf{T}(:,11)$ and $\mathbf{T}(:,12)$ are determined from the principal vector describing rigid body rotation about the y-axis, which is coupled to rigid body displacement in the z-direction, in the principal vector chain. For both of these rigid rotation pairs, all nodal forces are zero.

3.3.4. Bending moment pairs

The seventh and eighth columns $\mathbf{T}(:,7)$ and $\mathbf{T}(:,8)$ are termed a bending moment pair, and are determined from the principal vector describing a bending moment in the xy-plane, which is coupled to rigid body rotation about the z-axis, in the principal vector chain. The displacement components in the x-direction indicate not solely a bending curvature in the xy-plane, but rather rotations in the two principal planes and can be expressed in the form

$$\begin{bmatrix} d_{1x} \\ d_{2x} \\ d_{3x} \end{bmatrix}^{\mathbf{T}(:,7)} = a \times \begin{bmatrix} d_{1x} \\ d_{2x} \\ d_{3x} \end{bmatrix}^{\mathbf{T}(:,5)} + b \times \begin{bmatrix} d_{1x} \\ d_{2x} \\ d_{3x} \end{bmatrix}^{\mathbf{T}(:,11)}, \quad \begin{bmatrix} d_{4x} \\ d_{5x} \\ d_{6x} \end{bmatrix}^{\mathbf{T}(:,8)} = c \times \begin{bmatrix} d_{4x} \\ d_{5x} \\ d_{6x} \end{bmatrix}^{\mathbf{T}(:,6)} + d \times \begin{bmatrix} d_{4x} \\ d_{5x} \\ d_{6x} \end{bmatrix}^{\mathbf{T}(:,12)}. \tag{16}$$

Similarly, the 13th and 14th columns $\mathbf{T}(:,13)$ and $\mathbf{T}(:,14)$ are determined from a bending moment vector in the xz-plane which is coupled to rigid body rotation about the y-axis, in the principal vector chain. Again the displacement components in the x-direction can be decomposed as

$$\begin{bmatrix} d_{1x} \\ d_{2x} \\ d_{3x} \end{bmatrix}^{\mathbf{T}(:,13)} = e \times \begin{bmatrix} d_{1x} \\ d_{2x} \\ d_{3x} \end{bmatrix}^{\mathbf{T}(:,11)} + f \times \begin{bmatrix} d_{1x} \\ d_{2x} \\ d_{3x} \end{bmatrix}^{\mathbf{T}(:,5)}, \quad \begin{bmatrix} d_{4x} \\ d_{5x} \\ d_{6x} \end{bmatrix}^{\mathbf{T}(:,14)} = g \times \begin{bmatrix} d_{4x} \\ d_{5x} \\ d_{6x} \end{bmatrix}^{\mathbf{T}(:,12)} + h \times \begin{bmatrix} d_{4x} \\ d_{5x} \\ d_{6x} \end{bmatrix}^{\mathbf{T}(:,6)}. \tag{17}$$

Simple calculation from (16) and (17) gives the values of $a = -0.5$, $b = -0.2885$, $c = 0.5$, $d = -0.2885$; $e = -0.5$, $f = 0.2885$, $g = 0.5$ and $h = 0.2885$. The sign of the coefficients in the above decompositions allows one to characterise the nature of the coupling through interpretation of the cross-sectional rotations; for example, the two columns

$$\begin{bmatrix} d_{1x} \\ d_{2x} \\ d_{3x} \end{bmatrix}^{\mathbf{T}(:,5)} \quad \text{and} \quad \begin{bmatrix} d_{1x} \\ d_{2x} \\ d_{3x} \end{bmatrix}^{\mathbf{T}(:,11)}$$

represent rotations of the left-hand face of the cell about the y- and z-axes, respectively, while

$$\begin{bmatrix} d_{4x} \\ d_{5x} \\ d_{6x} \end{bmatrix}^{\mathbf{T}(:,6)} \quad \text{and} \quad \begin{bmatrix} d_{4x} \\ d_{5x} \\ d_{6x} \end{bmatrix}^{\mathbf{T}(:,12)}$$

are rotations of the right-hand face cell about the y- and z-axes, respectively; the fact that coefficients a and c are of equal magnitude but opposite sign indicates that this is a curvature in the xy-plane; on the other hand, the fact that coefficients b and d are equal indicates equal rotation of both faces of the cell, which is equivalent to a shear of the cell in the xz-plane. The nature of the above coupling has been confirmed through FEA of a ten-cell structure fixed at one end, and loaded at the other by a bending moment in the xy-plane distributed according to the nodal force components of the bending vector, $\mathbf{T}(:,8)$.

From the reciprocal theorem, just as a bending moment produces curvature, with a coupled shear deformation, so one would expect a shearing force to produce a shear deformation, with a coupled curvature; accordingly, the coupled equations for bending and shear in the two principal

planes are written as

$$M_z = EI_z/R_y + K_{xz}\gamma_{xz},$$
$$M_y = EI_y/R_z + K_{xy}\gamma_{xy}, \quad (18a, b)$$

$$Q_z = \kappa_{xz}AG\gamma_{xz} + K_{xz}/R_y,$$
$$Q_y = \kappa_{xy}AG\gamma_{xy} + K_{xy}/R_z, \quad (19a, b)$$

where K_{xz} and K_{xy} are the bending–shear coupling coefficients. The bending moment vector pairs **T**(:, 7) and **T**(:, 8), and **T**(:, 13) and **T**(:, 14) are shown in Figs. 5 and 6, respectively, from which the two bending curvatures in the xy- and xz-planes are $1/R_y = 1.443 \times 10^{-9}/(H/3 \times L/2) = 8.510 \times 10^{-8}\,\mathrm{m}^{-1}$, and $1/R_z = 2.5 \times 10^{-9}/(L/2 \times L/2) = 8.510 \times 10^{-8}\,\mathrm{m}^{-1}$; their coupled shear angles are $\gamma_{xz} = 1.443 \times 10^{-9}/(L/2) = 8.421 \times 10^{-9}$ in the xz-plane, and $\gamma_{xy} = 8.333 \times 10^{-10}/(H/3) = 8.421 \times 10^{-9}$ in the xy-plane, respectively. Note the absence of Poisson's ratio effects within these bending moment vectors.

3.3.5. *Shearing force pairs*

Finally, the ninth and 10th columns **T**(:, 9), and **T**(:, 10), and the 15th and 16th columns **T**(:, 15) and **T**(:, 16) of the transmission matrix describe the displacement and force components when the cell is subjected to both a shearing force and a bending moment in the xy- and xz-planes, respectively, and each is termed a *shearing force pair*. These pairs are determined from the two principal shear vectors in the xy- and xz-planes which are coupled with bending moments in the principal vector chains, and also coupled with the two bending vectors in the two orthogonal planes. The two shear pairs are shown in Figs. 7 and 8, but since a complete decomposition of the

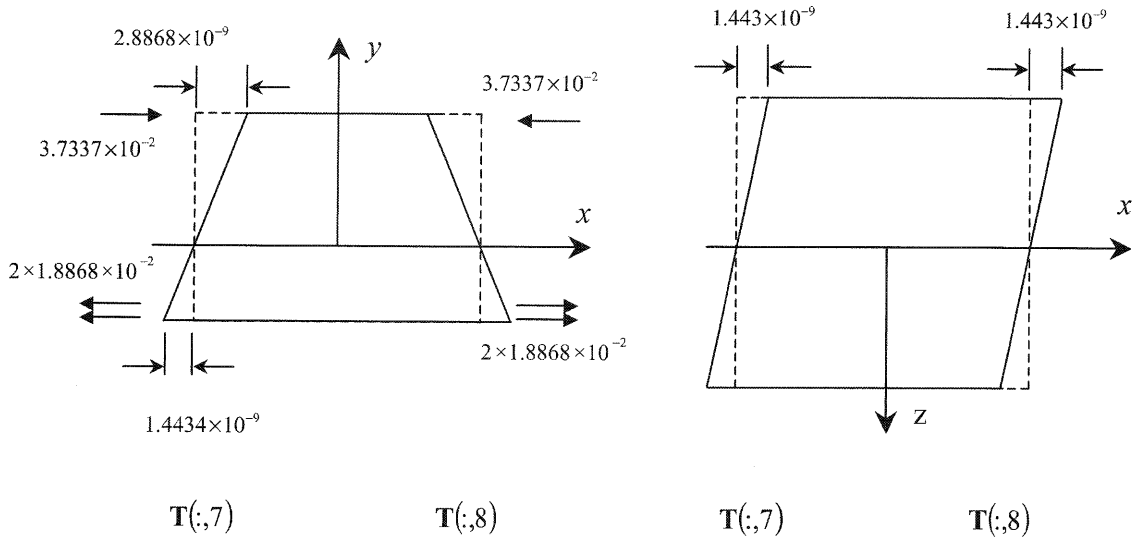

Fig. 5. Cell subject to pure bending moment in the xy-plane; vectors **T**(:,7) and **T**(:,8) describe the displacement and force components on the left- and right-hand sides of the cell, respectively.

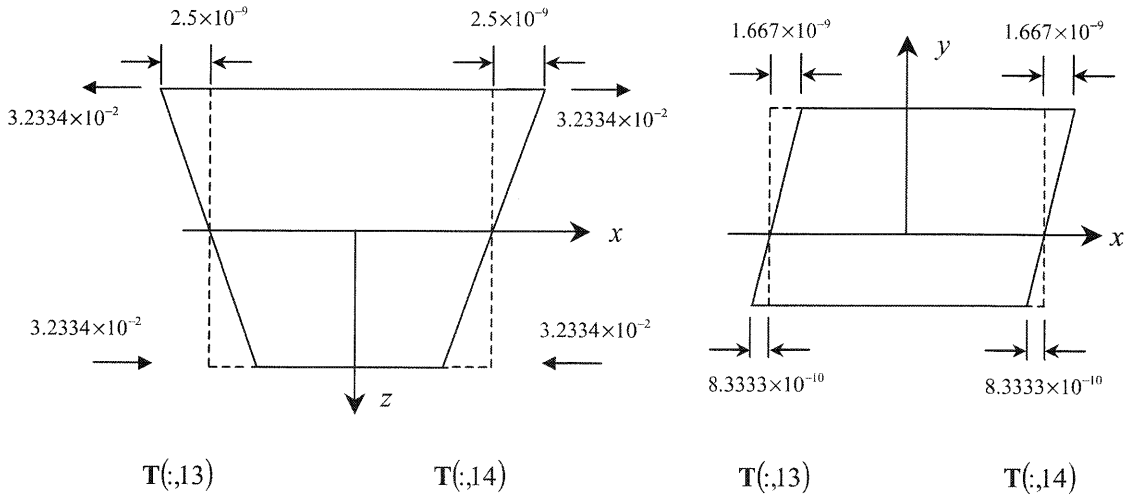

Fig. 6. Cell subject to pure bending moment in the xz-plane; vectors $\mathbf{T}(:,13)$ and $\mathbf{T}(:,14)$ describe the displacement and force components on the left- and right-hand sides of the cell, respectively.

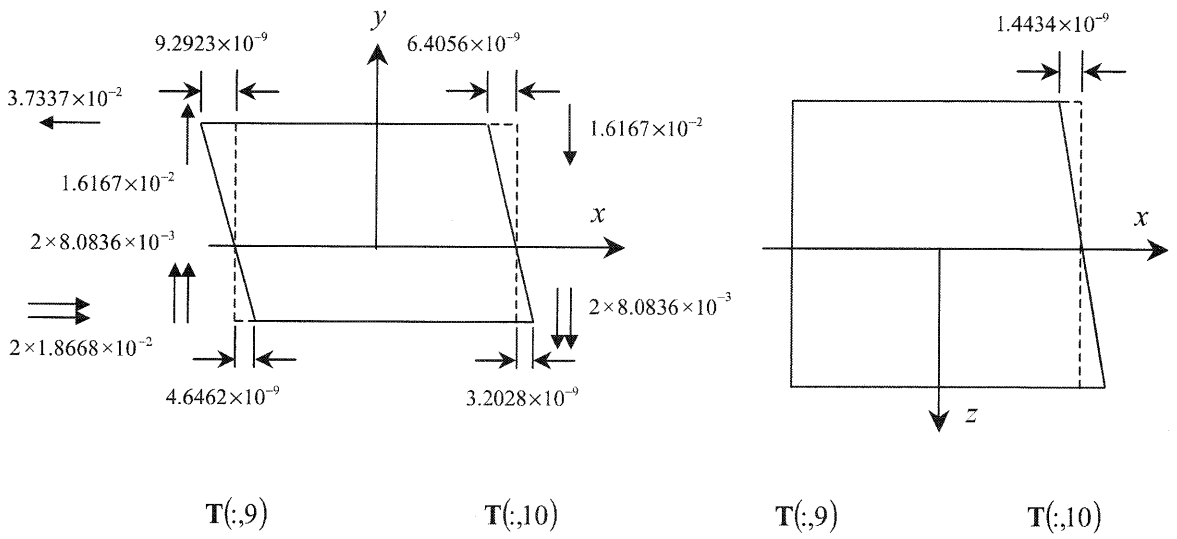

Fig. 7. Cell subject to shearing force and coupled bending moment in the xy-plane; vectors $\mathbf{T}(:,9)$ and $\mathbf{T}(:,10)$ describe the displacement and force components on the left- and right-hand side of the cell, respectively.

nodal displacements into equivalent cross-sectional displacements is rather involved, only the former is considered in detail, and shown in Figs. 9 and 10.

Within Timoshenko beam theory, the shear angle is defined according to the relationship $\gamma = \psi - \partial v/\partial x$, in which $\partial v/\partial x$ is the centreline slope and ψ is rotation of the cross-section. Now

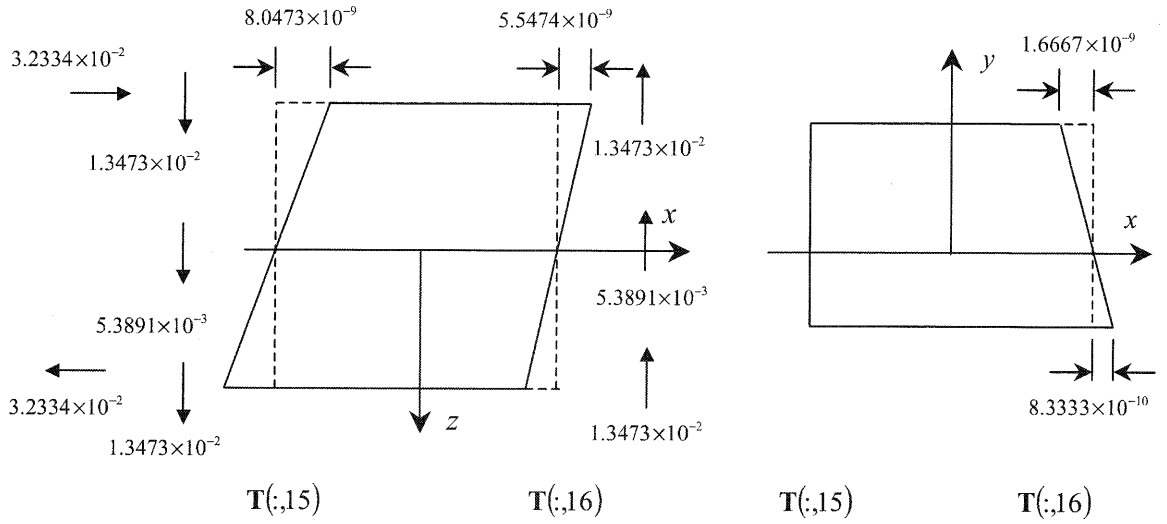

Fig. 8. Cell subject to shearing force and coupled bending moment in the xz-plane; vectors $\mathbf{T}(:,15)$ and $\mathbf{T}(:,16)$ describe the displacement and force components on the left- and right-hand side of the cell, respectively.

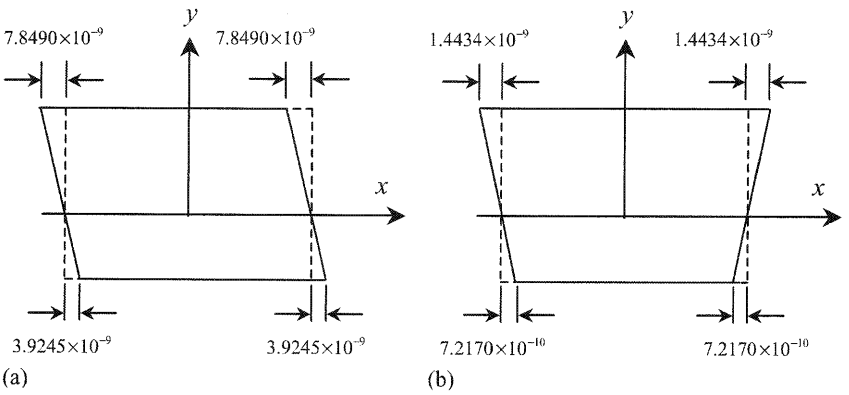

Fig. 9. Decomposition of the displacements of Fig. 7 in the xy-plane; (a) shows shear angle and (b) shows bending curvature.

since the centreline slope shown in Fig. 7 is already zero, one has $\partial v/\partial x = 0$, and from Fig. 9(a), equal cross-section rotations on both sides of the cell gives

$$\gamma_{xy} = 3.925 \times 10^{-9}/(H/3) = 3.966 \times 10^{-8}. \tag{20}$$

The coupled bending curvature is determined from Fig. 10(a) as

$$1/R_z = 7.217 \times 10^{-10}/(L/2 \times L/2) = 2.457 \times 10^{-8}\,\mathrm{m}^{-1}. \tag{21}$$

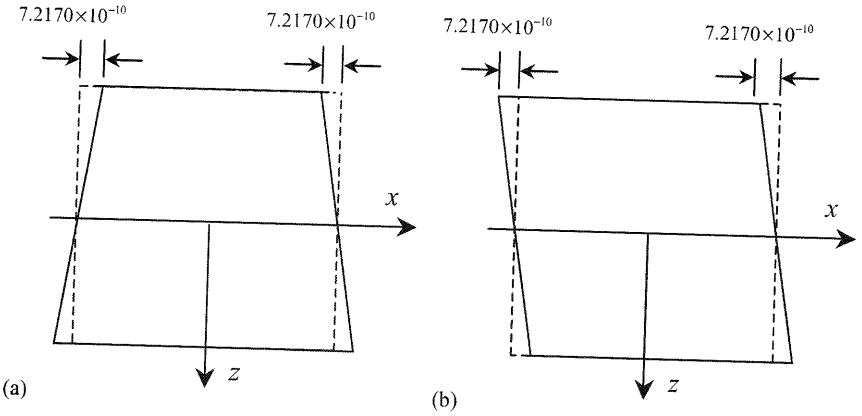

Fig. 10. Decomposition of displacements of Fig. 7 in the xz-plane; (a) shows bending curvature coupled with shear angle in the xy-plane due to shearing force, and (b) shows shear angle coupled with bending curvature in the xy-plane due to bending moment.

Now, since a shearing force on one side of the cell requires both a shearing force and a bending moment on the other—this equilibrium requirement is the physical interpretation of the principal vector chain—in turn, this *intrinsic* bending moment will give rise to secondary curvature and coupled shear for the cell; from Fig. 9(b), the secondary curvature is

$$1/R'_y = 7.217 \times 10^{-10}/(H/3 \times L/2) = 4.255 \times 10^{-8}\,\mathrm{m}^{-1} \tag{22}$$

and from Fig. 10(b), the secondary coupled shear angle in the perpendicular plane is

$$\gamma'_{xz} = 7.217 \times 10^{-10}/(L/2) = 4.211 \times 10^{-9}; \tag{23}$$

one sees that these secondary coupled displacements are precisely one-half of those produced by a pure bending moment in the xy-plane, Fig. 5. This is as one might expect: for a continuum, a shearing force produces a bending moment which varies linearly along the length of the cell, whose effect should be one-half that of the pure moment, the latter being constant along the length of the cell. These secondary effects become evident within a cell of finite length, but are not included within the coupled constitutive relationships, (19), which are applicable to a continuum element of infinitesimal length.

Having fully decomposed the nodal displacements into their cross-sectional equivalents, now evaluate the equivalent continuum properties: from Eqs. (18) and (19), the stiffness relationship for the bending and shear coupling of M_z and Q_z can be expressed in the matrix form

$$\begin{bmatrix} Q_z \\ M_z \end{bmatrix} = \begin{bmatrix} \kappa_{xz}AG & K_{xz} \\ K_{xz} & EI_z \end{bmatrix} \begin{bmatrix} \gamma_{xz} \\ 1/R_y \end{bmatrix}, \tag{24}$$

but it is more convenient to write this in its inverted form

$$\begin{bmatrix} \gamma_{xz} \\ 1/R_y \end{bmatrix} = \begin{bmatrix} n_{11} & n_{12} \\ n_{21} & n_{22} \end{bmatrix} \begin{bmatrix} Q_z \\ M_z \end{bmatrix} = \mathbf{N} \begin{bmatrix} Q_z \\ M_z \end{bmatrix}, \tag{25}$$

$$\begin{bmatrix}
4.646\times10^{-9} & 1.759\times10^{-9} & 5\times10^{-9} & 5\times10^{-9} & -3.333\times10^{-9} & 1.667\times10^{-9} & 8.047\times10^{-9} & 6.381\times10^{-9}\\
3.333\times10^{-9} & 3.333\times10^{-9} & 0 & 0 & 0 & 0 & 9.623\times10^{-10} & 9.623\times10^{-10}\\
0 & 0 & 0 & 1\times10^{-8} & 0 & 0 & -1.667\times10^{-9} & -1.667\times10^{-1}\\
4.646\times10^{-9} & 4.646\times10^{-9} & -5\times10^{-9} & -5\times10^{-9} & 1.667\times10^{-9} & -3.333\times10^{-9} & -8.047\times10^{-9} & -4.714\times10^{-9}\\
-3.333\times10^{-9} & -3.333\times10^{-9} & 0 & 0 & 0 & 0 & 9.623\times10^{-10} & 9.623\times10^{-10}\\
0 & 0 & 0 & 1\times10^{-8} & 0 & 0 & 1.667\times10^{-9} & 1.667\times10^{-9}\\
-9.292\times10^{-9} & -6.406\times10^{-9} & 0 & 0 & 1.667\times10^{-9} & 1.667\times10^{-9} & 0 & -1.667\times10^{-9}\\
0 & 0 & 0 & 0 & 0 & 0 & -1.925\times10^{-9} & -1.925\times10^{-9}\\
0 & 0 & 0 & 1\times10^{-8} & 0 & 0 & 0 & 0\\
-1.867\times10^{-2} & 0 & 0 & 0 & 3.233\times10^{-2} & 3.233\times10^{-2} & -3.233\times10^{-2} & 0\\
-8.084\times10^{-3} & -8.084\times10^{-3} & 0 & 0 & 0 & 0 & -4.667\times10^{-3} & -4.667\times10^{-3}\\
-4.667\times10^{-3} & -4.667\times10^{-3} & 0 & 0 & 0 & 0 & -1.347\times10^{-2} & -1.347\times10^{-2}\\
-1.867\times10^{-2} & 0 & 0 & 0 & -3.233\times10^{-2} & -3.233\times10^{-2} & 3.233\times10^{-2} & 0\\
-8.084\times10^{-3} & -8.084\times10^{-3} & 0 & 0 & 0 & 0 & 4.667\times10^{-3} & 4.667\times10^{-3}\\
4.667\times10^{-3} & 4.667\times10^{-3} & 0 & 0 & 0 & 0 & -1.347\times10^{-2} & -1.347\times10^{-2}\\
3.734\times10^{-2} & 0 & 0 & 0 & 0 & 0 & 0 & 0\\
-1.617\times10^{-2} & -1.617\times10^{-2} & 0 & 0 & 0 & 0 & 0 & 0\\
0 & 0 & 0 & 0 & 0 & 0 & -5.389\times10^{-3} & -5.389\times10^{-3}
\end{bmatrix}.$$

Appendix B. Tension and torsion pairs

$$\textbf{[Tension]} = \begin{bmatrix}
0 & 1\times10^{-8}\\
0 & \sqrt{3}\times10^{-8}\\
0 & -1\times10^{-8}\\
0 & 1\times10^{-8}\\
0 & -\sqrt{3}\times10^{-8}\\
0 & -1\times10^{-8}\\
0 & 1\times10^{-8}\\
0 & 0\\
0 & 2\times10^{-8}\\
6.467\times10^{-2} & 6.467\times10^{-2}\\
0 & 0\\
0 & 0\\
6.467\times10^{-2} & 6.467\times10^{-2}\\
0 & 0\\
0 & 0\\
6.467\times10^{-2} & 6.467\times10^{-2}\\
0 & 0\\
0 & 0
\end{bmatrix}, \quad \textbf{[Torsion]} = \begin{bmatrix}
0 & 1.025\times10^{-9}\\
-2.958\times10^{-10} & 8.274\times10^{-9}\\
-5.124\times10^{-10} & -5.460\times10^{-9}\\
0 & 1.025\times10^{-9}\\
-2.958\times10^{-10} & -8.866\times10^{-9}\\
5.124\times10^{-10} & -4.436\times10^{-9}\\
0 & 1.025\times10^{-9}\\
5.916\times10^{-10} & 5.916\times10^{-10}\\
0 & 9.896\times10^{-9}\\
0 & 0\\
2.870\times10^{-3} & 2.870\times10^{-3}\\
-1.657\times10^{-3} & -1.657\times10^{-3}\\
0 & 0\\
-2.870\times10^{-3} & -2.870\times10^{-3}\\
-1.657\times10^{-3} & -1.657\times10^{-3}\\
0 & 0\\
0 & 0\\
3.313\times10^{-3} & 3.313\times10^{-3}
\end{bmatrix}.$$

References

[1] The official NASA photograph ID is STS61B-120-052. http://images.jsc.nasa.gov/index.html.
[2] Stephen NG, Wang PJ. On Saint-Venant's principle in pin-jointed frameworks. International Journal of Solids and Structures 1996;33:79–97.
[3] Noor AK. Continuum modelling for repetitive lattice structures. ASME Applied Mechanics Reviews 1988;42:285–96.
[4] Sun CT, Kim BJ. Continuum modelling of periodic truss structures. In: Damage mechanics and continuum modelling. Detroit, Michigan: ASCE Convention; 1985. p. 57–71.
[5] Lee U. Dynamic continuum modelling of beamlike space structures using finite element matrices. AIAA Journal 1990;28:725–31.
[6] Love AEH. Mathematical theory of elasticity, 4th ed. New York: Dover Publications; 1944.
[7] Lekhnitskii SG. Theory of elasticity of an anisotropic elastic body. San Francisco: Holden-Day; 1963.